Proc. Schl. Eng. Tokai Univ., Ser. E
43 (2018) 1-7

A Study on Corona Discharge Characteristics with Stratified Dielectric Plate under AC High Voltage

by

Ny SOCHINLY[*1,2] and Ryu-ichiro OHYAMA[*3]

(Received on Mar. 26, 2018 and accepted on July 5, 2018)

Abstract

Gas insulation apparatuses must be monitored in order to detect local dielectric deterioration caused by electrical damages such as corona discharge. In this work, the electrical characteristics of a current pulse signal from corona discharge in atmospheric air were examined. The corona discharge was observed in a needle-to-plate electrode system. The geometry of the electrode gap was varied by using a stratified dielectric plate (glass plate) to form the surface and barrier corona discharge fields. An experiment was conducted in order to investigate the influence of either the dielectric surface of the barrier on the corona discharge characteristics. The experimental methods were based on the phase resolved partial discharge (PRPD) pattern and V-Q Lissajous figure. The current pulse magnitude i_p, repetition number n and charge quantity Q_w of the corona discharge field are discussed for different electrode gap geometries.

Keywords: Corona discharge, Electrode gap geometry, Stratified dielectric plate, Needle-to-plate electrode, AC high voltage

1. Introduction

"Corona discharge" is a nomenclature of partial discharge (PD) in high voltage gas-insulation system. It is easy to occur around the sharp place of electrode surface in high voltage apparatuses. Usually, an appropriate solid insulator such as dielectric barrier substances compounds with the electrode system, in the purpose to support mechanically the electrode in the gas insulation and to prevent electrically the breakdown of the whole electrode gap. The dielectric solid parts in the gas insulation system are extensively used in high voltage electrical apparatuses, such as bushing-type insulators and transformers. The well design of dielectric substance parts enhances the insulation performance and raises the corona inception voltage (PDIV) in air gap [1)]. Although the barrier substance improves the dielectric strength for the breakdown of the gas insulation, the insulating arrangements may often cause the PD phenomenon in term of surface and barrier corona discharges. These corona discharges affect the degradation of insulation system with long term. One means to examine a sign of the insulation degradation is an effective monitoring of the current pulse signal emitted from the corona discharge. Regarding to this current pulse signal, numerous researchers have been achieved [2-6)]. A means of quantitative evaluations required for the corona discharge detection and monitoring is expected even now. However, the matter is that how should we manage the appropriate insulation constitution to prevent corona discharge degradation. The corona discharge is an unwanted phenomenon of high voltage insulation system, which may lead to failure of equipment. As a result, it's required costly and time-consuming maintenance or replacing whole components. Accordingly, one means to examine a sign of the insulation degradation is an age sampling evaluation on the corona discharge. In the conventional study for AC corona discharge, there are many examples which demanded PDIV [7)], characteristics of corona current pulse magnitude i_p and repetition number n [8)] and numerical modeling of corona discharge [9)].

A stratified dielectric plate arranged in electrode gap performs to prevent the breakdown of the whole electrode gap. The spatial development of ionization process induces the PD phenomenon of dielectric surface. The boundary condition of the dielectric plate changes the characteristic of corona discharge. In the monitoring of the corona discharge, it is always expected where is the incident part of the invisible corona discharge. In order to examine the influence of either dielectric surface of the barrier on PD characteristics in the

*1 Graduate Student, Course of Electrical and Electronic Engineering
*2 Electricity of Cambodia
*3 Professor, Dept. of Electrical and Electronic Engineering.

atmospheric air, the experiment in this work was conducted by two methods of phase resolved partial discharge (PRPD) pattern and V-Q Lissajous figure. From a quantitative point of view, this report discusses the current pulse number *n,* current pulse magnitude i_p and charge quantity Q_w as the corona discharge characteristics with a stratified dielectric plate for different electrode gap geometries.

2. Experimental Setup

2.1 *Electrode gap geometry*

Fig. 1 shows the explanatory test object with different electrode gap geometry in the experiment. The electrode system consists of a brass needle electrode of 0.8 mm, a brass plate electrode of 70 mm in diameters. The tip of the needle electrode was spherically rounded as a point and acted as a corona discharge electrode. In this experiment, three corona discharge fields varied in the arrangement of a dielectric plate were tested; (a) corona discharge without dielectric plate, (b) surface corona discharge, and (c) barrier corona discharge. The plate was a glass of 80 mm in diameter, 0.7 mm in thickness. The electrode gap length in the atmospheric air was 5 mm in (a) and (c) approximately.

2.2 *Measurements*

Fig. 2 shows the explanatory circuit for measurements of (a) current pulse number *n* and current pulse magnitude i_p, and (b) charge quantity Q_w of corona discharge. The applied voltage waveform *v(t)* from an AC high-voltage source (50 Hz) to the needle-to-plate electrode system was recorded to an oscilloscope (350Hz, 2GS/s) via a high-voltage divider (HVD; Sohei, 330MΩ, 3pF). The signal *i(t)* of i_p was detected by a

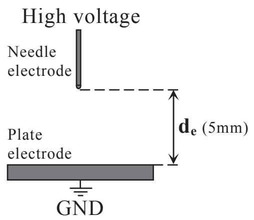

(a) Type of corona discharge without dielectric plate.

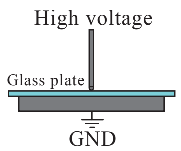

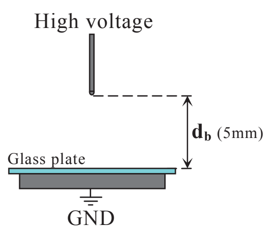

(b) Type of surface discharge. (c) Type of barrier discharge.

Fig. 1 Electrode gap geometry.

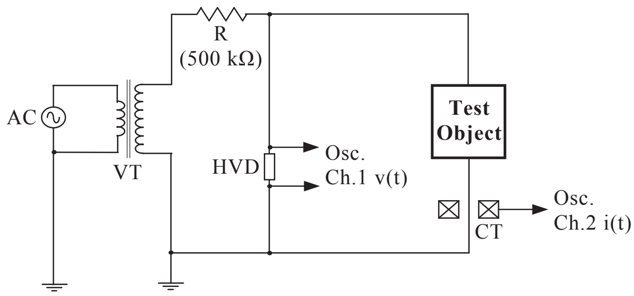

(a) Setup for PRPD pattern.

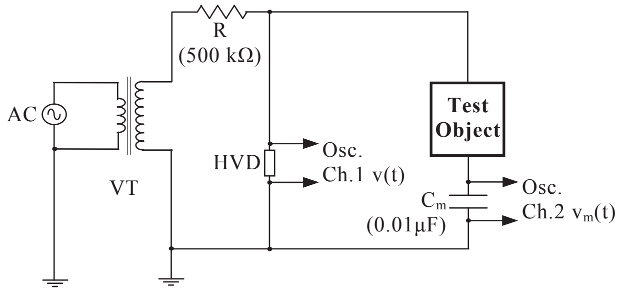

(b) Setup for V-Q Lissajous figure.

Fig. 2 Explanatory circuit for measurements.

current transformer (CT; Tektronix, CT-1) and recorded to the oscilloscope as shown in (a). The charge quantity Q_w on the glass plate surface was analyzed from the V-Q Lissajous figure, in which the value of Q_w as a function of the applied voltage was recorded to oscilloscope as shown in (b). The value of Q_w was detected between the both ends of a condenser C_m (0.01μF) connected in series to the electrode gap.

3. Results and Discussions

3.1 *Phase resolved partial discharge (PRPD) patterns*

PRPD patterns are widely used to recognize the types of PD and identify the insulation properties [10-15]. In this work, the PRPD patterns were used to analyze the statistical characteristics of current pulse signal. Fig. 3 shows the typical PRPD patterns of corona discharge observed from the electrode gap as shown in Fig. 1 (a), where the applied voltage V_p are 5.31 kV (PDIV) in (a), and 6.87 kV in (b). At inception voltage of 5.31 kV in peak value, the corona current pulses appeared in the negative voltage half-cycles, see (a). With increasing voltage, the positive corona current pulses could be seen. Fig. 4 shows the PRPD patterns of surface corona discharge as shown in Fig. 1 (b). At inception voltage of 1.25 kV, the corona current pulses on both half-cycles appeared, see (a). The number of pulses were enhanced with increasing voltage, see (b). Fig. 5 shows the PRPD patterns of barrier corona discharge as shown in Fig. 1 (c). The characteristic

(a) V_p=5.31 kV.

(b) V_p=6.87 kV.

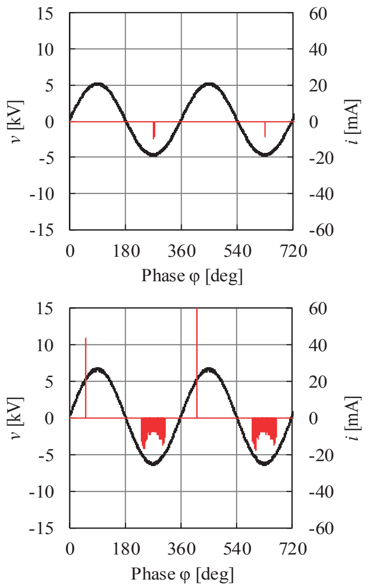

Fig. 3 PRPD patterns of corona discharge.

(a) V_p=1.25 kV.

(b) V_p=7.18 kV.

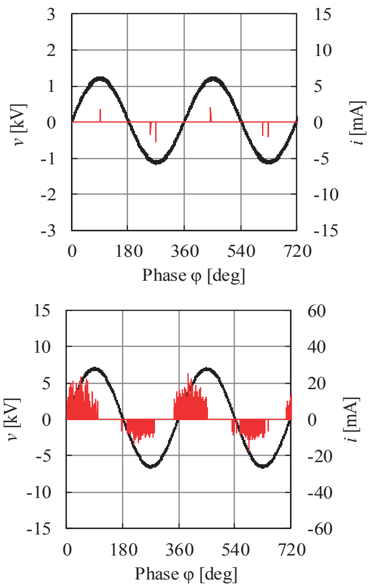

Fig. 4 PRPD patterns of surface corona discharge.

(a) V_p=5.93 kV.

(b) V_p=7.34 kV.

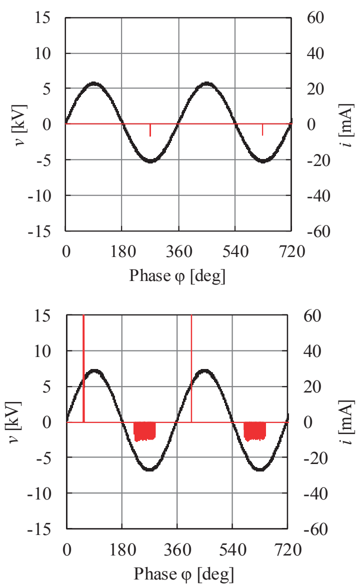

Fig. 5 PRPD patterns of barrier corona discharge.

was as somewhat similar to the case as shown in Fig. 3. However, it's necessary to notice that the PRPD pattern of barrier corona discharge is significantly depended on the air gap length d_b between electrode and dielectric substance. If the air gap d_b is too short, the PRPD pattern of barrier corona discharge becomes similar characteristic as surface corona discharge phenomenon.

From the point of view of corona discharge characteristics, it is necessary to comprehend the behavior of ion space charge. The ion space charge (negative ion such as O_2^- and/or positive ion such as N_2^+) in corona discharge fields behaves as a residual charge to the electrode gap or an accumulated charge on the surface of dielectric solid substances. Normally, the ion space charge has been discussed under the condition of DC applied voltage rather than AC [16-19]. The theoretical difference between AC and DC corona charges is the presence of periodic polarity inverse in the direction of electric field. An effective electric field strength enhances around the ion space charge, because the outer electric field (E_{out}) based on applied voltage and the internal electric field (E_{int}) on ion space charge are superimposed. In AC corona discharge, the electric field strength depending on the phase of applied voltage cycle remarkably changes by the polarity and quantity of ion space charge induced from the preceding half-cycle. The ion space charge of barrier corona discharge may properly understand from that of corona discharge. Hence, only ion space charge of corona discharge can be discussed as follow.

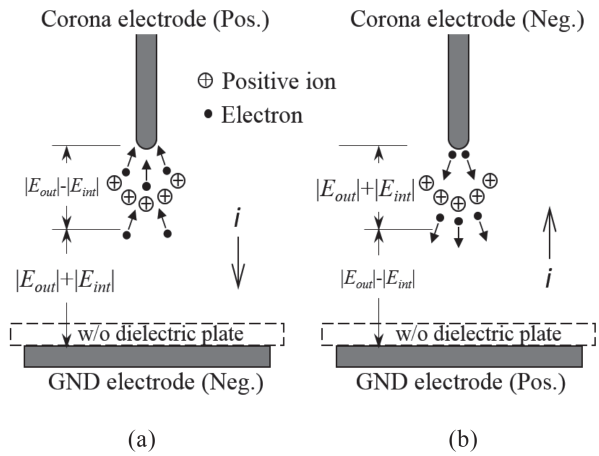

Fig.6 Explanation of ion space charge in corona discharge field.

As shown in Fig.6, when the applied voltage polarity of corona discharge electrode is positive (a), the corona discharge starts from a required primary electron depending on the process of electronic avalanche. Taking into account the fundamental ionization mechanism of the Townsend discharge, the free electron accelerates towards the positive corona electrode, and produces a positive ion pair from the ionization process. The mobility of electron is 10^3 to 10^4 times of ion mobility in atmospheric air. The electron is absorbed to the positive electrode and the positive ion remains in the neighborhood of the positive electrode. In respect of the behavior of positive ion such as N_2^+, a quantitative evaluation by the numerical computation is often tried, because the experimental evaluation is considerably difficult [20]. The electronic avalanche makes a positive space charge region surrounding the positive corona electrode. As the result, the effective electric field strength ($|E_{out}|$ - $|E_{int}|$) is reduced between the positive corona electrode and positive space charge region. Between the positive space charge region and opposite electrode in the ground, the strength ($|E_{out}|$ + $|E_{int}|$) is enhanced on the contrary. Therefore, in the positive corona discharge, the onset voltage depending on $|E_{out}|$ - $|E_{int}|$ and current pulse magnitude on $|E_{out}|$ + $|E_{int}|$ are increased relatively. The number n of corona current pulses is equivalent to the number of streamer progressed from the electronic avalanche. As shown in Fig.3 (b), the current pulse is relatively high-magnitude i_p and low-number n, because the streamer progresses from the positive space charge region to opposite electrode side for a relative long way. On the other hand, when the applied voltage polarity of corona discharge electrode is negative shown in Fig.6 (b), the corona discharge starts from the tip of electrode. The free electron accelerates towards the ground electrode and produces a positive ion pair from the electronic avalanche. A positive space charge region is formed around the negative corona electrode. As the result, the effective electric field strength ($|E_{out}|$ + $|E_{int}|$) is enhanced between the negative corona electrode and positive space charge region. Between the positive space charge region and opposite electrode in the ground, the strength ($|E_{out}|$ - $|E_{int}|$) is reduced. Therefore, in the negative corona discharge, the onset voltage depending on $|E_{out}|$ + $|E_{int}|$ and current pulse magnitude on $|E_{out}|$ - $|E_{int}|$ are decreased relatively. As shown in Fig.3 (b), the current pulse is relatively low-magnitude i_p and high-number n, because the streamer progresses from the positive space charge region to corona discharge electrode for a relative short way.

3.2 *Corona discharge characteristics on n and i_p*

Fig. 7 shows the corona current pulse number n in average (a) and corona current pulse magnitude i_p in maximum (b) from the electrode gap as shown in Fig. 1 (a), where each plot is statistical value per two cycles. The characteristics are presented as a function of applied voltage V_p in peak value. The values of n and i_p have a polarity effect causing to positive ion space charge as mentioned above. The pulse number n of negative corona discharge means a relative short way in an

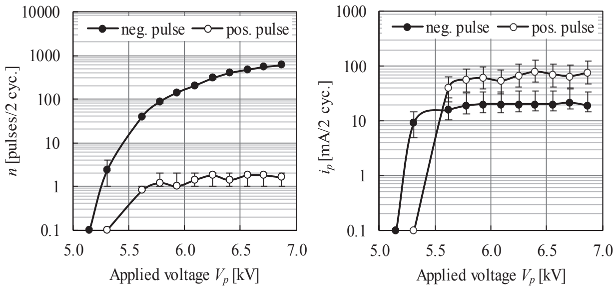

(a) Number n. (b) Magnitude i_p.

Fig. 7 Characteristic of corona discharge.

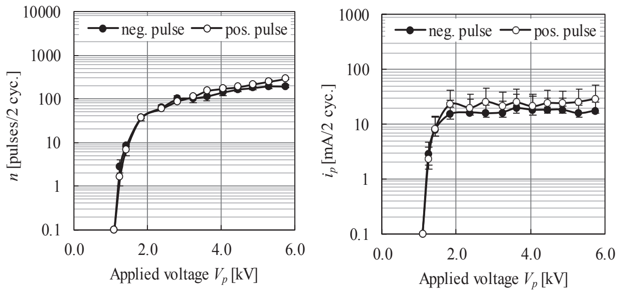

(a) Number n. (b) Magnitude i_p.

Fig. 8 Characteristic of surface corona discharge.

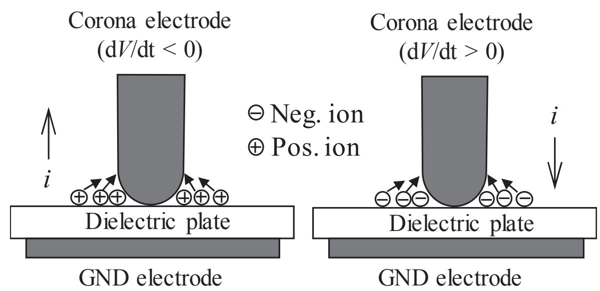

Fig. 9 Explanation of accumulated ion space charge in surface corona discharge.

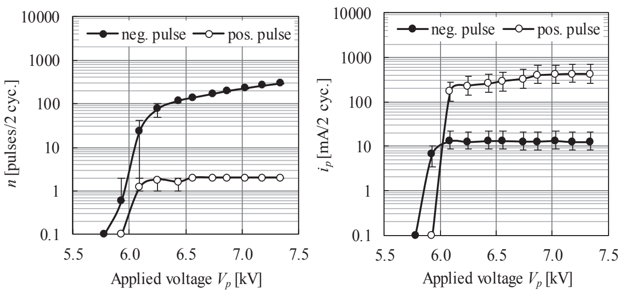

(a) Number n. (b) Magnitude i_p.

Fig. 10 Characteristic of barrier corona discharge.

active region between the positive space charge and corona discharge electrode. Also, the pulse magnitude i_p of positive corona discharge means a relative long way in an active region between the positive space charge and grounded electrode side. Fig. 8 shows the characteristics of n and i_p from the surface corona discharge case as shown in Fig. 1 (b). The characteristics of surface corona discharge are quite different from the corona discharge with non-dielectric plate mentioned above. Whenever the polarity of applied voltage changes in period, the polarity of ions accumulated on the surface of dielectric plate is turned (see Fig. 9). When the polarity of the applied voltage turns over, the accumulation ions remarkably emphasize the effective electric field strength. Therefore, the polarity difference is neglected, because the generation phase of surface corona discharge is close to zero-cross of applied voltage as shown in Fig. 4 (b). Around the phase of zero-cross (such as 0, 180 deg.) the electric field strength is increased as an interaction of ion space charge and corona discharge electrode with polarity different each other. As shown in Fig.9, with closing to the zero-cross in dV/dt < 0 phase (90 to 270 deg.) after positive discharge, the effective electric field strength ($|E_{out}|$ + $|E_{int}|$) with the residual positive ion accumulated on the dielectric plate reaches to the corona onset. As the result, the negative surface corona discharge appears. In succession, the positive surface corona discharge with the accumulated negative ion appears in dV/dt > 0 phase (270 to 450 deg.). For the corona discharge phenomena in atmospheric air, it is common in the electrostatic charge on the surface of dielectric plate to use as expression of the ions instead of electrons. The negative ions are as a result of electron attachment into the atmospheric molecules such as O_2 and a cluster such as H_2O. Fig. 10 shows the characteristics of n and i_p from the barrier corona discharge case as shown in Fig. 1 (c). The result is as somewhat similar to characteristics as shown in Fig. 7.

Fig. 11 shows the combination of above characteristics to see the similarity for different electrode gap geometry. The characteristics of corona discharge with non-contacted electrode to the glass plate are almost similar in “corona” and “barrier”. The onset voltage of surface corona discharge is relatively lower, because the negative and/or positive ion accumulated on the glass plate enhances the electric field strength for following polarity inverse of applied voltage cycle. Thus, the surface corona discharge could be distinguished from other AC corona discharge cases.

3.3 *Charge quantity Q_w on V-Q Lissajous figure*

Fig. 12 shows a typical V-Q Lissajous figure from the electrode gap as shown in Fig. 1 (b). A parallelogram shape

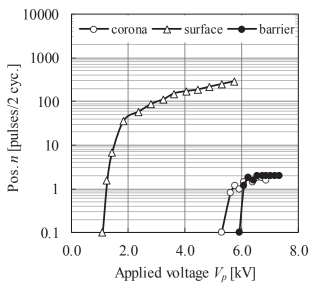

(a) n in positive.

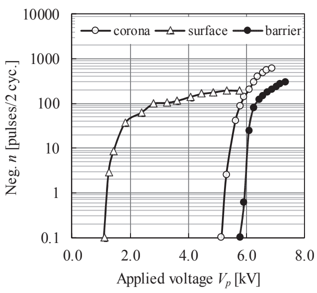

(b) n in negative.

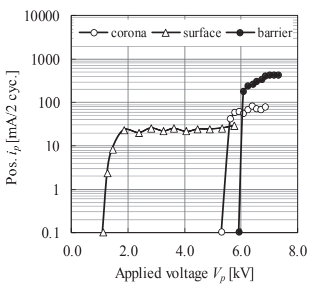

(c) i_p in positive.

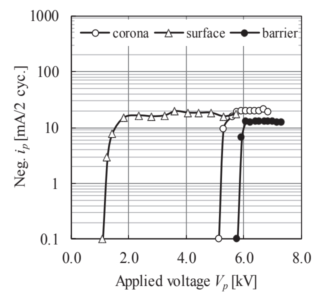

(d) i_p in negative.

Fig. 11 Characteristic of corona discharge w/o stratified dielectric plate.

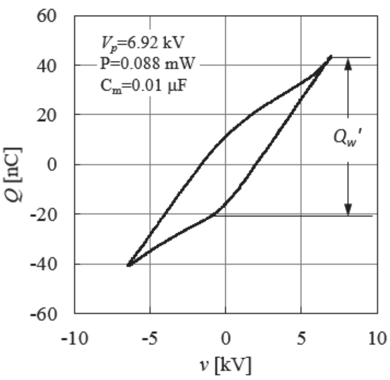

Fig. 12 Typical V-Q Lissajous figure from surface corona discharge.

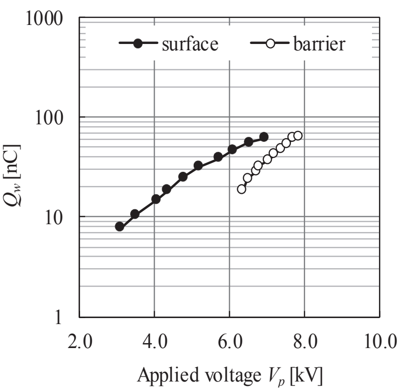

Fig. 13 Charge quantity Q_w as a function of V_p in surface and barrier corona discharges.

Table 1 Q_w of surface and barrier corona discharges.

Surface corona discharge		Barrier corona discharge	
V_p [kV]	Q_w [nC]	V_p [kV]	Q_w [nC]
1.2 (PDIV)	—	5.9 (PDIV)	—
6.3	49.8	6.3	18.3
6.5	55.3	6.5	24.1

figure drawn on unclockwise rotation consists of two regions w/o PD. The charge quantity Q_w accumulated on the glass plate and discharge power intensity can be obtained from this figure, respectively [21-24]. Fig. 13 shows the charge quantity Q_w as a function of applied voltage V_p from the electrode gap as shown in Fig. 1 (b) and (c). The charge quantity Q_w can be calculated from the following expression;

$$Q_w = Q_w' \frac{1}{1+C_s/C_d} \qquad (1)$$

where Q_w' is the apparent quantity obtained from the V-Q Lissajous figure (see Fig. 12), C_s is the stray capacitance, and C_d is the capacitance of electrode gap. It is known that the values of Q_w depending to V_p are almost same order for the surface and barrier corona discharges. Table 1 shows the values of Q_w as a function of applied voltage V_p. Although the inception voltage of surface corona discharge is lower than that of barrier corona discharge, at same applied voltage (V_p = 6.3 ~ 6.5 kV), Q_w of surface corona discharge is higher than those of barrier corona discharge. From the point of insulation degradation view, the monitoring of Q_w is an effective procedure for evaluation of dielectric performance [25,26]. Accordingly, it is thought that the accumulation of quantitative characteristic will be useful in future.

4. Conclusions

The corona discharge on different electrode gap geometry to simplify gas insulation apparatuses was experimentally examined. The characteristics of current pulse number n, current pulse magnitude i_p and charge quantity Q_w of the corona discharge fields were evaluated with a stratified dielectric plate arranged in electrode gap. The characteristics were discussed in the term of behavior on ion space charge as residual charge to the electrode gap or accumulated charge on the surface of stratified dielectric plate.

References

1) V. N.Maller and K.D.Srivastava, "Corona Inception and Breakdown in Nonuniform Field with Insulating Support in Air," IEEE Transactions on Industry Applications, **IA-23**, 5, pp.820-824 (1987).
2) A.A.Arainy, N.H.Malik and M.K.Bahloul, "Statistical variation of AC corona pulse amplitudes in point-to-plane air gaps," IEEE Transactions on Electrical Insulation, **24**, 4, pp.681-687 (1989).
3) B.Florkowska and R. Wlodek, "Pulse height analysis of partial discharges in air," IEEE Transactions on Electrical Insulation, **28**, 6, pp.932-940 (1993).
4) W.He, Y.Wang, L.Lan, X.Wen and B.Wan, "Characteristics of AC corona discharge pulses and RI levels in a coaxial wire-cylinder gap," *IEEE International Conference on High Voltage Engineering and Application (ICHVE),* pp.1-4 (2016).
5) M.Nemamcha, "Effect of a dielectric plate on the discharge in needle to plane system submitted to AC voltage," *Eleventh International Symposium on High Voltage Engineering, London,* Vol.3, pp.175-178 (1999).
6) E.Jahoda, L.Varačka, J.Kúdelčík and M.Kúdelčíková, "Study of the surface discharge on the air-insulation interface," *2016 ELEKTRO*, Strbske Pleso, pp. 616- 619 (2016).
7) S.Yanabu and Y.Kawaguchi, "Calculation of AC Corona Inception Voltage Under Non-Uniform Field Air Gaps", Transactions on IEE Japan, **91**, 8, pp.1543-1550 (1971).
8) K.Okumura, "An Investigation of AC Corona Pulse and Noise Produced by Needle to Plane Gap in Air", Transactions on IEE Japan, **110-A**, 1, pp.59-68 (1990).
9) R.Tirumala and D.B.Go, "Comparative study of corona discharge simulation techniques for electrode configurations inducing non-uniform electric fields", Journal of Electrostatics, **72**, pp.99-106 (2014).
10) H.Illias, T.S.Yuan, A.H.A. Bakar, H.Mokhlis, G.Chen and P.L.Lewin, *"Partial discharge patterns in high voltage insulation", IEEE International Conference on Power and Energy (PECon),* pp.750-755 (2012).
11) C.Hudon and M.Belec, "The importance of phase resolved partial discharge pattern recognition for on-line generator monitoring," *Conference Record of the 1998 IEEE International Symposium on Electrical Insulation (Cat. No.98CH36239),* Vol.1, pp.296-300 (1998).
12) C.Hudon and R.H. Rehder, "Recognition of phase resolved partial discharge patterns for internal discharges and external corona activity," *Proceedings of 1995 IEEE 5th International Conference on Conduction and Breakdown in Solid Dielectrics*, Leicester, pp. 386-392 (1995).
13) T.Joyo, T.Okuda, N.Kadota, R.Miyatake, S.Okada and K.Mio, "Phase resolved partial discharge patterns for various damage of winding insulation detected with different measuring devices," *IEEE Electrical Insulation Conference (EIC),* pp.344-347 (2017).
14) T.Tanmaneeprasert, P.L.Lewin and G.Callender, "Analysis of degradation mechanisms of silicone insulation

containing a spherical cavity using partial discharge detection," *IEEE Electrical Insulation Conference (EIC)*, pp.233-236 (2017).

15) *IEEE Standard for High-Voltage Switchgear (Above 1000 V) Test Techniques – "Partial Discharge Measurements,"* IEEE Std, C37.301-2009, pp.55-61 (2009).

16) P.S.Maruvada, *"Corona Performance of High-voltage Transmission Lines,"* Research Studies Press Ltd., p.67-76 (2000).

17) F.A.M.Rizk and G.N.Trinh, *"High Voltage Engineering,"* Taylor & Francis Group, LLC., 2014, p.189-210.

18) E.Kuffel, W.S.Zaengl and J.Kuffel, *"High Voltage Engineering: Fundamentals,"* Butterworth-Heinemann, p.349-359 (2000).

19) M.Khalifa, *"High Voltage Engineering Theory and Practice,"* MARCEL DEKKER, INC., p.123-131 (1990).

20) A.Ohsawa,"Computer simulations of insulator charge neutralisations with a corona ioniser - Influence of initial surface charge distribution", Journal of Electrostatics, **71**, pp.287-293 (2013).

21) G.Yulin et al., "Electric parameter measurement of dielectric barrier discharge," *12th IEEE International Conference on Electronic Measurement & Instruments (ICEMI),* pp.631-636 (2015).

22) Y.Z.Sun, Y.C.Qiu and F.F.Li, "Calculation of dielectric barrier discharge parameters using Lissajous diagram," Journal of Henan Polytechnic University. **24**., pp.113-115 (2005).

23) Z.Cheng, F.Zhi, J.Hu, L.Zhao and Y.Qiu, "Simulation and experiment study on dielectric barrier discharge under different conditions," Zhongguo Dianji Gongcheng Xuebao/Proceedings of the Chinese Society of Electrical Engineering. **28**, pp.33-39 (2008).

24) T.Tamida, A.Iwata and M.Tanaka, "Discharge Measurement of ac Plasma Display Panels using V-Q Lissajous' Figure," IEEJ Transactions on Fundamentals and Materials, **118**, pp.353-358 (1998).

25) J.You, Z.Jia, Y.Wang, W.Fan, Y.Yuan and Z.Guan, "Evaluation analysis of XLPE cable's electrical condition," *IEEE Conference on Electrical Insulation and Dielectric Phenomena*, pp.470-473 (2014).

26) F.Wester, E.Gulski, J.J.Smit, P.N.Seitz and M.Turner, "Application of advanced PD diagnostics for condition-based maintenance of MV power cable systems," *Conference Record of the IEEE International Symposium on Electrical Insulation (Cat. No.00CH37075)*, pp. 115-118 (2000).